ISSN 2278-2540 | DOI: 10.51583/IJLTEMAS | Volume XV, Issue VI, June 2026

Influence of Cerium (Ce) Doping on the Optical Properties of Silver Telluride (Ag_2Te) Thin Films Deposited by Electrodeposition Method.

Okafor Lois Ugomma[1*], Okafor Anthony Amaechi[2] , Abonyi Sylvester Emeka[3]

[1]Department of Physics and industrial physics, Nnamdi Azikiwe University, Awka Anambra State, Nigeria

[2]Department of Mechanical Engineering, Nnamdi Azikiwe University, Awka AnambraState, Nigeria

[3]Department of Electrical Engineering, Nnamdi Azikiwe University, Awka Anambra State, Nigeria

[*]Corresponding Author

DOI: https://doi.org/10.51583/IJLTEMAS.2026.150600246

Received: 12 July 2026; Accepted: 17 July 2026; Published: 01 August 2026

ABSTRACT

In this investigation, Silver telluride (Ag_2Te) thin films have been successfully deposited onto FTO glass substrate using electro deposition method to investigate the influence of Ce doping on optical properties of Ag_2Te films. Silver trioxonitrate (V) and tellurium (iv) oxide were the precursors used for silver and tellurium ions. Depositions of films made from cerium-doped silver telluride were conducted at room temperature. The percentages concentration of cerium dopant used in this investigation are 2.5%, 5.0%, 7.5% and10.0%. The optical properties of the thin films were characterized using Uv-Vis spectrometry. Absorbance results confirm that increasing Ce concentration significantly increases the absorbance of Ag_2T films across the UV, VIS, and NIR regions. The 10.0% Ce-doped sample demonstrates the highest absorbance across all regions, with values of 43.36% at 365 nm, 42.68% at 400 nm, 34.00% at 700 nm, and 35.16% at 1100 nm, indicating the strong influence of cerium in enhancing light absorption. This trend reflects that as Ce concentration increases, absorbance improves significantly in all spectral regions, suggesting that Ce doping introduces additional localized states that facilitate electronic transitions, thereby enhancing the films' optical properties. The transmittance of Ag_2Te and Ce-doped Ag_2Te films decreases notably with increasing cerium concentration across the UV, VIS, and NIR regions. This decline in transmittance with increasing Ce concentration is consistent with the corresponding increase in absorbance suggesting that Ce doping enhances light absorption, thus reducing the amount of light transmitted through the films. Cerium doping enhances reflectance slightly, particularly in the NIR regions, likely due to increased surface roughness and scattering effects introduced by Ce incorporation. The extinction coefficient (k) of silver telluride and cerium-doped silver telluride films generally increases with wavelength, indicating higher optical absorption at longer wavelengths. Other optical results were also presented.

Keywords: Silver Telluride, optical properties, Electrodeposition. Cerium doping Spectrophotometer

INTRODUCTION

Silver telluride (Ag_2Te) is a chalcogenide semiconductor composed of silver (Ag) and tellurium (Te), belonging to group iv-vi compounds on the periodic table [1] which exhibit semiconductor properties. In bulk form, it crystallizes in a monoclinic $\beta-$ phase at room temperature and undergoes a phase transition to a cubic $\alpha-$ phase at elevated temperatures, approximately 423k [2], with associated changes in electrical behavior. Ag_2Te exhibits n-type conductivity and has been studied for magneto resistance and thermo electric applications [2]. Nanostructured forms of silver telluride, such as quantum dots or nanorods , show enhanced properties due to

ISSN 2278-2540 | DOI: 10.51583/IJLTEMAS | Volume XV, Issue VI, June 2026

quantum confinement effects, including increased band gaps and strong photoluminescence within infrared range, which differs greatly from bulk materials [3]. These nanostructures are synthesized by different methods such as hydrothermal processes or chemical deposition, using precursors such as $AgNO_3$ and $TeCl_4$ [4]. Recently, Ag_2Te quantum dots have emerged as heavy metal-free alternatives to traditional chalcogenide nano materials, giving tunable optoelectronic properties for near-infrared (NR) and shortwave infrared (SWIR) photodetectors with competitive responsivity and detectivity [3]. Besides optoelectronics, the compound finds application in non linear optical devices, ion-selective electrodes, electrochemical storage cells, solar cells and biological sensors, stating its versatility in energy, environmental and sensing technologies [2]. Reports from literature [6, 7, 8, 9] showed no information on the influence of dopant concentration on the optical properties of cerium doped silver telluride films. The purpose of this research is to address the literature gap by investigating the influence of concentration of cerium doping on the optical properties of silver telluride films synthesized via electrodeposition. Specifically, we aim to elucidate how different dopant concentration influences the optical properties of electrodeposited Ag_2Te films.

Experimental

Reagents

Reagents used for electrodeposition of cerium doped silver telluride $(Ce: AgTe)$ were; Silver trioxonitrate (V): used as precursor for silver ion., Cerium tetraoxosulphate (VI) tetrahydrate: used as precursor for cerium ion (dopant ion), Tellurium (IV) oxide: used as precursor for tellurium ion, ethylene diamine tetra acetic acid (EDTA): used as a complexing agent, distilled water was used as solvent.

Apparatus

The experimental arrangement shown in section 4, Figure 1 [5] illustrates the setup for electrodeposition, comprising the electrolyte, power supply unit, and electrodes. It adopts a three-electrode configuration for depositing thin films onto conducting substrates. The conducting substrate, specifically FTO, was used as the cathode or working electrode. A platinum electrode functioned as the anode or counter electrode, while a silver/silver chloride (Ag/AgCl) electrode served as the reference electrode. The energy supply for the electrodeposition setup is provided by a Dazheng digital DC-power supply unit, specifically the PS-1502A model. Two digital multimeters, the DT9201A CE and the highly sensitive Mastech: MY60 were employed for measuring voltage and current, respectively. The Mastech: MY60 multimeter is capable of measuring currents within the range of 10^{-6} A.

Material preparation

Molar solutions of the reagents prepared for the deposition include:

Silver trioxonitrate (V)

Silver trioxonitrate (V) is an inorganic compound with chemical formula $AgNO_3$. It is a versatile precursor to many other silver compounds. It is a colorless salt with molar mass of 169.87 g/mol. About 256 g of the salt is soluble in 100 mL at 25 °C. In this work, silver trioxonitrate (V) served as precursor for Ag ion and various concentrations (0.10 M and 0.01 M) of silver trioxonitrate (V) was prepared by dissolving particular amount of the compound in 100 ml of distilled water.

Cerium tetraoxosulphate (VI) tetrahydrate

Cerium (IV) tetraoxosulphatetetrahydrate, also called ceric sulfate, is an inorganic compound with chemical formula ($Ce(SO_4)_2 . 4H_2O$). The salt is a yellow solids that are moderately soluble in water and dilute acids. Solutions of ceric sulfate have a strong yellow color. It has a molar mass of 404.30 g/mol. In this work, 0.01 M of the salt was prepared by dissolving 0.40 g in 100 mlof distilled water

ISSN 2278-2540 | DOI: 10.51583/IJLTEMAS | Volume XV, Issue VI, June 2026

Tellurium (IV) oxide

Tellurium (IV) oxide, also known as tellurium dioxide (TeO_2) is a white crystalline solid with molecular weight of 159.60 g/mol and it is negligible soluble in water. Tellurium (IV) oxide served as precursor for tellurium ion. In this work, 0.20 mole solution of TeO_2 was prepared by dissolving 7.98 g in 250 ml of distilled water.

Diluted tetraoxosulphate (VI) acid solution

H_2SO_4 has a molar mass of 98.079 g/mol. 1.0 M of H_2SO_4 was prepared by adding 55.60 ml of 96 % concentrated H_2SO_4 to 1000 ml of distilled water. The 55.60 ml of H_2SO_4 was obtained by using the percentage concentration of the H_2SO_4 (96%), molar mass of H_2SO_4 (98.079 g/mol) and specific density of (1.84 g/ml). The diluted H_2SO_4 served as pH adjuster

Substrate pre-treatment

Prior to electrodeposition of the films, the FTO substrates were subjected to distinct pre – treatment to ensure the presence of catalytic surface to improve the adhesion of the films to the substrates most especially when there is possibility of increase in film thickness as deposition proceeds. This pre – treatment of FTO glass substrates was achieved through the following six steps;

(i) We cleaned the FTO glass substrates with detergents.

(ii) We soaked the substrates in acetone for 10 minutes for degreasing.

(iii) We ultrasonicated the substrates for 20 minutes in an ultrasonic bath using ethanol as a solvent.

(iv) We ultrasonicated the substrates for 10 minutes in an ultrasonic bath using distilled as a solvent.

(v) We rinsed the substrates twice with distilled water.

(vi) We dried the substrates in an electronic oven for 10 minutes at a temperature of about 100℃.

Electrodeposition

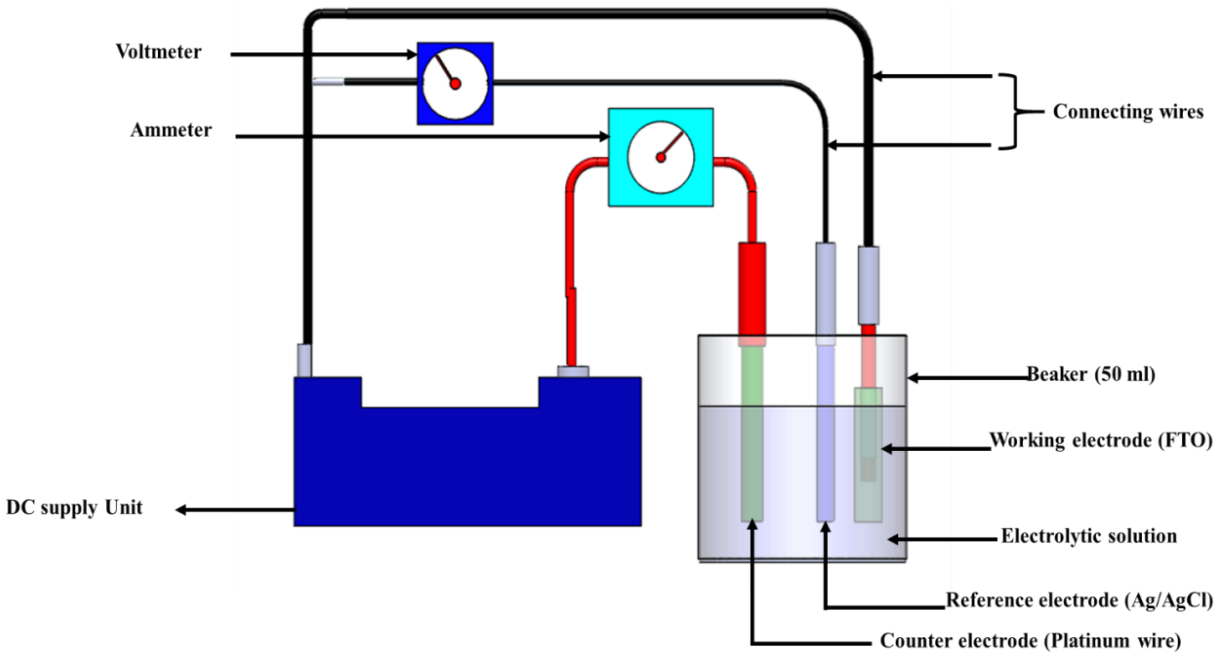

Figure 1: Schematic diagram of the electrodeposition experimental set – up [5]

ISSN 2278-2540 | DOI: 10.51583/IJLTEMAS | Volume XV, Issue VI, June 2026

Depositions of thin films made from cerium-doped silver chalcogenide (Ce:Ag_2Te) were conducted at room temperature. Molar concentration bath parameter of the cerium precursor was adjusted to optimize their impact on the optical characteristics of these films.

Electrodeposition of silver telluride and cerium doped silver telluride($Ce:Ag_2Te$) thin films

For electrodeposition of silver telluride thin film on FTO substrate, aqueous electrolytic bath composed of 20ml of 0.10 M of silver trioxonitrate (V) and 5 ml of 1.0 M of H_2SO_4 were poured into the electrolytic bath. The mixture was stirred for 5 minutes. This was followed by addition of 15 ml of 0.1 M of tellurium (IV) oxide solution to the mixture. This followed with another stirring for 5 minutes. After stirring, the three electrodes were immersed into the bath containing the electrolytic solution and 2 volts was allowed to pass through the setup for 15 seconds. After the allowed time, grey film of Ag_2Te was found to be deposited on the conductive surface of the FTO substrate. The deposited Ag_2Te thin film was heat-treated at 100 ℃ for 10 minute to remove water and improve the crystallinity of the deposited thin films. The mechanism of the formation of silver telluride and cerium doped silver telluride is shown in equation (1) and (2).

$$2Ag^{+} + Te^{4+} + 2e^{-} \longrightarrow Ag_2Te \qquad 1$$

Optimization of Ce ion concentration for $Ce:Ag_2Te$ thin films

For the deposition of Ce doped Ag_2Te thin films, 0.05 M of cerium (IV) tetraoxo sulphate tetrahydrate was used as dopant source. Similar procedure used for deposition of silver telluride thin film was adopted but with addition of different volume concentrations of 0.05 M of cerium (IV) tetraoxosulphate tetra hydrate as shown in Table 1. Four samples with different dopant volume concentrations of 1 ml, 2 ml, 3 ml and 4 ml were fabricated.

$$2Ag^{+} + Te^{4+} + Ce^{4+} + 2e^{-} \longrightarrow Ce:Ag_2Te \qquad 2$$

Table 1: Bath parameter for deposition of Ag_2Te and Ce doped Ag_2Te thin films

0.10 M of $AgNO_3$	**0.10 M of TeO_2**	**0.05 M of $CeSO_4 \cdot 4H_2O$**	**1.0 M of H_2SO_4**	**Applied Voltage**	**Time**
Vol. (ml)	Vol. (ml)	Vol. (ml)	Vol. (ml)	(volts)	(sec.)
20.00	15.00	-	5.00	2.00	15
20.00	15.00	1.00	5.00	2.00	15
20.00	15.00	2.00	5.00	2.00	15
20.00	15.00	3.00	5.00	2.00	15
20.00	15.00	4.00	5.00	2.00	15

Characterization of deposited thin films

The fabricated thin films were characterized to determine their optical properties using spectrophotom

eter, Thickness measurements of the films were carried out using gravimetric method

Film thickness measurement

The deposited film thicknesses (t) were evaluated using the gravimetric method given by [10]; [11]; [12].

$$t = \frac{\Delta m}{\rho A}, \qquad 3$$

ISSN 2278-2540 | DOI: 10.51583/IJLTEMAS | Volume XV, Issue VI, June 2026

In equation (3),Δm is the mass of the film. A is the surface area of the deposited film and ρ is the bulk density of the material film. The masses of the deposited films were obtained by finding the difference in mass between the mass of the glass substrate with the film after deposited and the mass of glass substrate before deposition. These differences in mass of the films were measured using analytical weighing balance with sensitivity of 0.0001 g.

Bulk density of Ag_2Te is 8.32 g/cm^3. Bulk density of cerium is 8.16 g/cm^3. Because of small amount of cerium impurity used and possibility of cerium ions to substitute silver in the crystal structure, density of Ce:Ag_2Te was approximated to bulk density of Ag_2Te.

Optical characterization

The optical absorbance of the films deposited was obtained using spectrophotometer (model: 756S UV – VIS) at Nano Research Laboratory, Department of Physics and Astronomy, University of Nigeria Nsukka, Enugu State, Nigeria. Other optical properties of the films such as transmittance, reflectance, refractive index, extinction coefficient, real dielectric constant, imaginary dielectric constant and energy band gap were evaluated using the formulae below;

Transmittance of the film was evaluated using equation (4) given by [13; 14]

$$T = 10^{-A} \quad (4)$$

Reflectance was obtained using the expression in equation (5) as given by [15; 16].

$$R = 1 - [T \cdot exp(A)]^{\frac{1}{2}} \quad (5)$$

The absorption coefficient (α) was calculated from the transmittance values using the equation (6) as given by [17; 18; 19].

$$\alpha = \frac{1}{t}\left(\frac{1}{T}\right). \quad (6)$$

Where t is the thickness of the film obtained using equation (3) above.

Extinction coefficient was obtained using equation (7) as given by [20; 21; 22].

$$k = \frac{\alpha \lambda}{4\pi} \quad (7)$$

Refractive indices of the films were calculated using equation (8) as given by [23;24; 25].

$$\eta = \frac{1+R}{1-R} + \sqrt{\frac{4R}{(1-R)^2} - k^2} \quad (8)$$

Optical conductivity was estimated using equation (9) as given by [26].

$$\sigma_o = \frac{\alpha \eta c}{4\pi}. \quad (9)$$

Where c is the speed of light.

The energy band gap was estimated using Tauc's model of equation (10) as given by [20]

$$(\alpha h v)^n = \beta\left(hv - E_g\right). \quad (10)$$

Where β is a constant, $n = 2$ for direct band gap. The energy band gaps of the films were obtained by extrapolating the straight portion of the plot of $(\alpha hv)^2$ against the photon energy (hv) at$(\alpha hv)^2 = 0$.

ISSN 2278-2540 | DOI: 10.51583/IJLTEMAS | Volume XV, Issue VI, June 2026

RESULTS AND DISCUSSIONS

Optical Properties of Ag_2Te and cerium doped Ag_2Te thin films

Variation of optical properties Ag_2Te with percentage concentration of cerium dopant

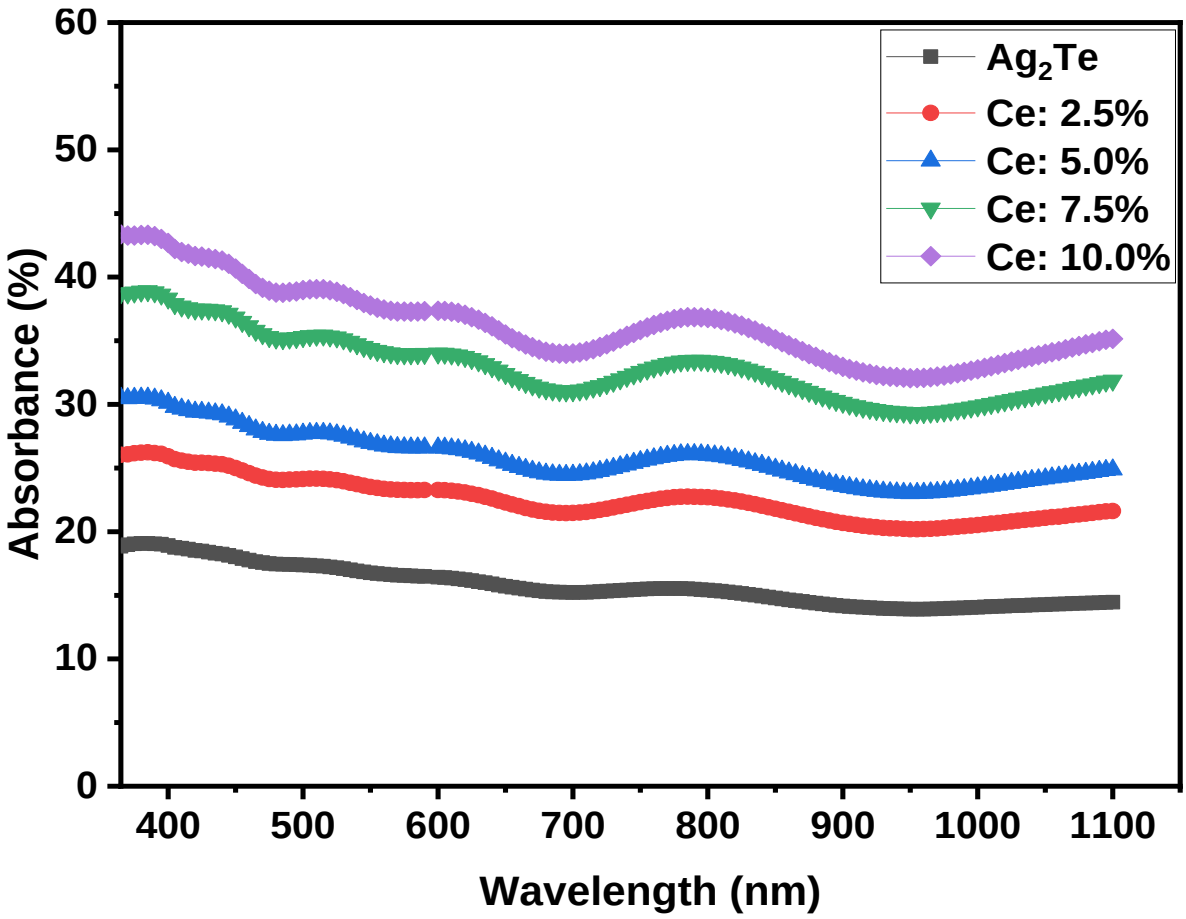

Figure 2: Plot of absorbance against wavelength for silver telluride and cerium doped silver telluride thin films deposited at different concentration of cerium ion precursor

As shown in Figure 2, the absorbance of Ag_2Te and Ce-doped Ag_2Te thin films varies significantly across the UV, VIS, and NIR regions, with notable differences among the samples. For pure Ag_2Te, the absorbance starts at 18.85% at 365 nm, slightly increases to 18.92% at 400 nm, and continues to decline to 15.22% at 700 nm and 14.45% at 1100 nm, indicating a gradual reduction in photon absorption as wavelength increases. With 2.5% Ce doping, absorbance increases to 26.04% at 365 nm, 25.92% at 400 nm, 21.47% at 700 nm, and 21.62% at 1100 nm, showing enhanced absorption compared to pure Ag_2Te, particularly in the UV and VIS regions. The 5.0% Ce-doped sample exhibits further improvement, with absorbance reaching 30.52% at 365 nm, 30.12% at 400 nm, 25.46% at 700 nm, and 26.88% at 1100 nm, highlighting the effect of increased Ce concentration on optical activity. At 7.5% Ce doping, absorbance rises to 38.73% at 365 nm, 38.33% at 400 nm, 34.04% at 700 nm, and 31.87% at 1100 nm, showing a substantial increase, especially in the VIS and NIR regions. The 10.0% Ce-doped sample demonstrates the highest absorbance across all regions, with values of 43.36% at 365 nm, 42.68% at 400 nm, 34.00% at 700 nm, and 35.16% at 1100 nm, indicating the strong influence of cerium in enhancing light absorption. This trend reflects that as Ce concentration increases, absorbance improves significantly in all spectral regions, suggesting that Ce doping introduces additional localized states that facilitate electronic transitions, thereby enhancing the films' optical properties.

ISSN 2278-2540 | DOI: 10.51583/IJLTEMAS | Volume XV, Issue VI, June 2026

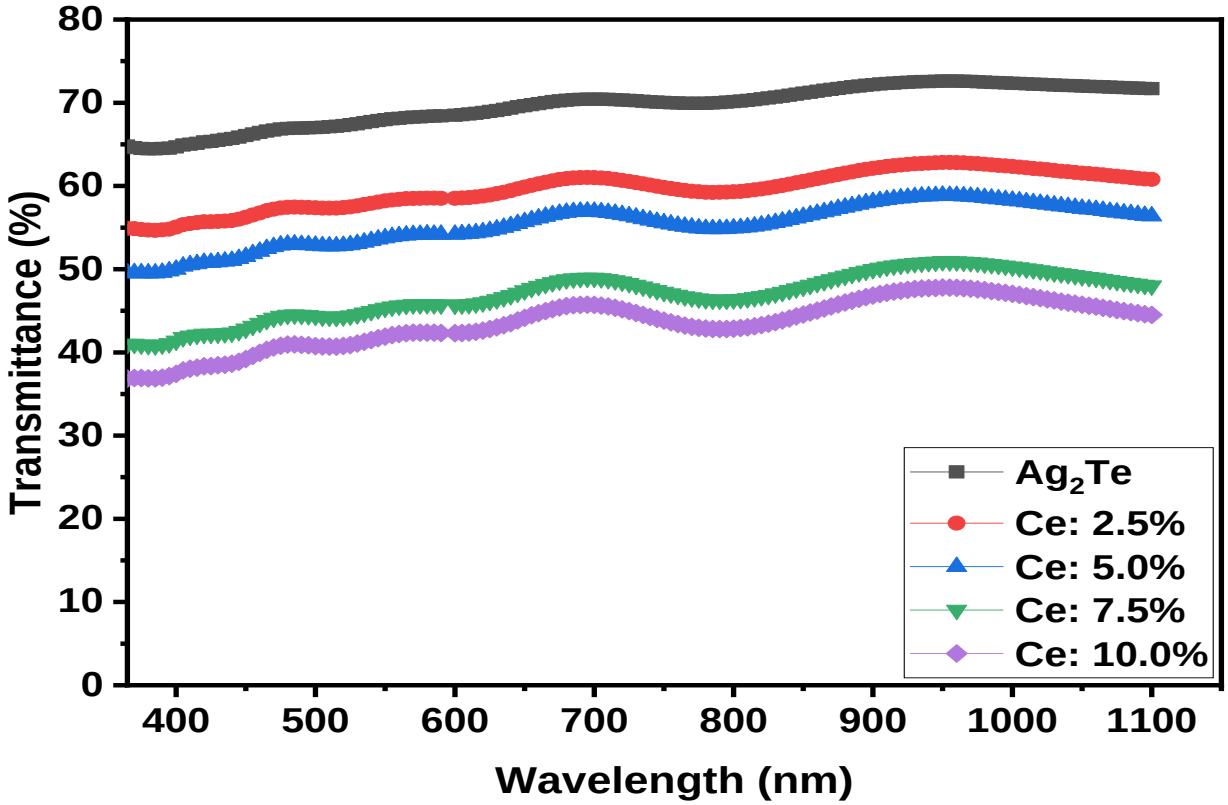

Figure 3: Plot of transmittance against wavelength for silver telluride and cerium doped silver telluride thin films deposited at different concentration of cerium ion precursor

As illustrated in Figure 3, the transmittance of Ag_2Te and Ce-doped Ag_2Te thin films decreases notably with increasing cerium concentration across the UV, VIS, and NIR regions. For pure Ag_2Te, the transmittance is highest, starting at 64.79% at 365 nm, slightly decreasing to 64.69% at 400 nm, and increasing to 70.44% at 700 nm and 71.69% at 1100 nm which indicate higher transparency in the longer wavelength regions. When doped with 2.5% Ce, the transmittance drops to 54.90% at 365 nm, 55.05% at 400 nm, 61.00% at 700 nm, and 60.79% at 1100 nm, reflecting reduced transparency compared to pure Ag_2Te. At 5.0% Ce doping, transmittance further decreases to 49.52% at 365 nm, 49.97% at 400 nm, 56.93% at 700 nm, and 53.38% at 1100 nm. This trend continues with 7.5% Ce doping, where transmittance values are 40.99% at 365 nm, 41.37% at 400 nm, 48.93% at 700 nm, and 44.00% at 1100 nm, showing significant reduction, especially in the NIR region. The 10.0% Ce-doped sample exhibits the lowest transmittance across all wavelengths, with 36.85% at 365 nm, 37.43% at 400 nm, 45.71% at 700 nm, and 44.51% at 1100 nm. This decline in transmittance with increasing Ce concentration is consistent with the corresponding increase in absorbance suggesting that Ce doping enhances light absorption, thus reducing the amount of light transmitted through the films.

As shown in Figure 4, the reflectance of Ag_2Te and Ce-doped Ag_2Te thin films varies moderately with both wavelength and cerium concentration. For pure Ag_2Te, the reflectance decreases slightly from 16.39% at 365 nm to 16.25% at 400 nm, then reduces further to 14.34% at 700 nm and 13.86% at 1100 nm, indicating lower reflection at longer wavelengths. Upon doping with 2.5% Ce, reflectance increases to 19.06% at 365 nm, 19.03% at 400 nm, 17.53% at 700 nm, and 17.59% at 1100 nm, showing an overall increase compared to pure Ag_2Te. With 5.0% Ce doping, the reflectance values are 19.96% at 365 nm, 19.90% at 400 nm, 18.60% at 700 nm, and 18.73% at 1100 nm, indicating a slight rise across the spectrum. For the 7.5% Ce-doped film, reflectance continues to increase, reaching 20.28% at 365 nm, 20.30% at 400 nm, 20.03% at 700 nm, and 20.12% at 1100 nm. At the highest doping level of 10.0% Ce, reflectance stabilizes around 19.79% at 365 nm, 19.89% at 400 nm, 20.29% at 700 nm, and 20.34% at 1100 nm. This trend suggests that cerium doping enhances reflectance slightly, particularly in the NIR regions, likely due to increased surface roughness and scattering effects introduced by Ce incorporation.

ISSN 2278-2540 | DOI: 10.51583/IJLTEMAS | Volume XV, Issue VI, June 2026

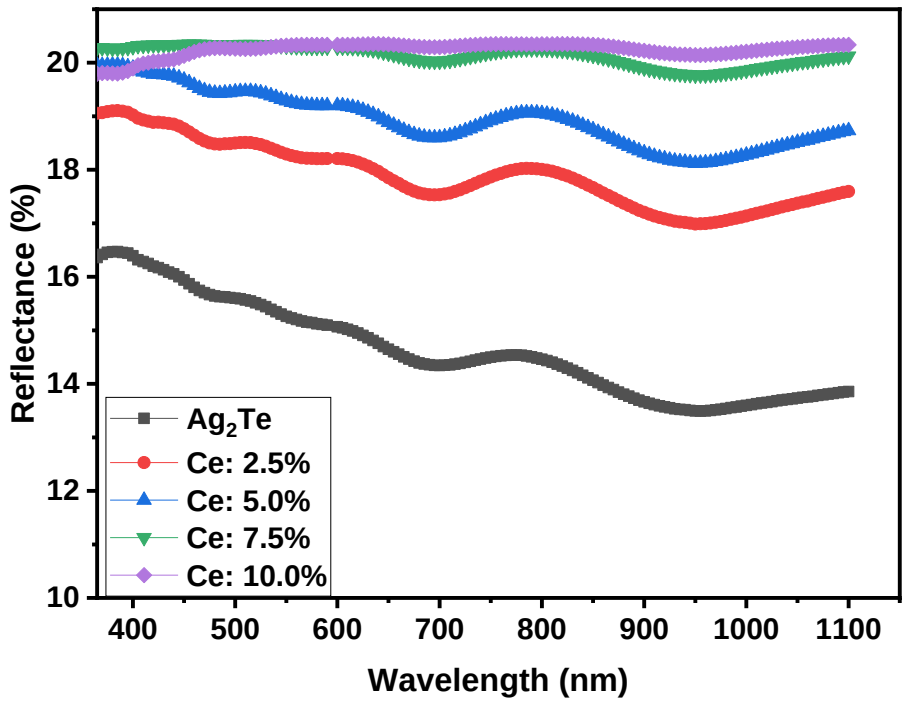

Figure 4: Plot of reflectance against wavelength for silver telluride and cerium doped silver telluride thin films deposited at different concentration of cerium ion precursor

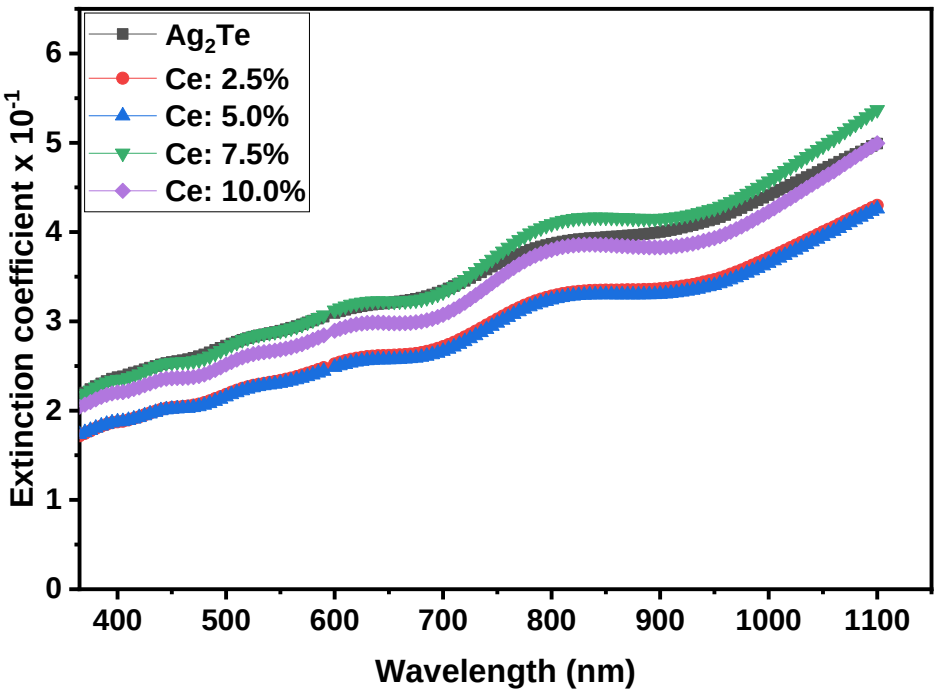

Figure 5: Plot of extinction coefficient against wavelength for silver telluride and cerium doped silver telluride thin films deposited at different concentration of cerium ion precursor

The extinction coefficient commonly denoted as k in the context of optics and electromagnetism is a measure of how strongly a material absorbs light at a given wavelength. The extinction coefficient (k) of silver telluride and cerium-doped silver telluride thin films, as shown in Figure 5, generally increases with wavelength, indicating

ISSN 2278-2540 | DOI: 10.51583/IJLTEMAS | Volume XV, Issue VI, June 2026

higher optical absorption at longer wavelengths. For pure Ag_2Te, k increases from 2.16×10^{-1}at 365 nm to 4.99×10^{-1}at 1100 nm, showing a strong wavelength-dependent absorption. At 2.5% cerium doping, k starts lower at 1.72×10^{-1} but rises to 4.30×10^{-1} at 1100 nm, suggesting reduced absorption at shorter wavelengths but a comparable response at higher wavelengths. Similarly, the 5.0% doped film exhibits a lower extinction coefficient of 1.73×10^{-1} at 365 nm, which increases to $4.26\times10^{-1}10^{-1}$at 1100 nm. The 7.5% doped sample follows a slightly different trend, starting at 2.17×10^{-1} at 365 nm and reaching a peak of 5.37×10^{-1} at 1100 nm, the highest among the samples, indicating enhanced light absorption in the infrared region. The 10.0% doped film shows an intermediate response with k values of 2.04×10^{-1} at 365 nm and 4.99×10^{-1} at 1100 nm, similar to pure Ag_2Te. The trend suggests that doping influences optical absorption by modifying carrier concentration and defect states. The lower extinction coefficient at shorter wavelengths for doped films indicates improved transparency in the UV region.

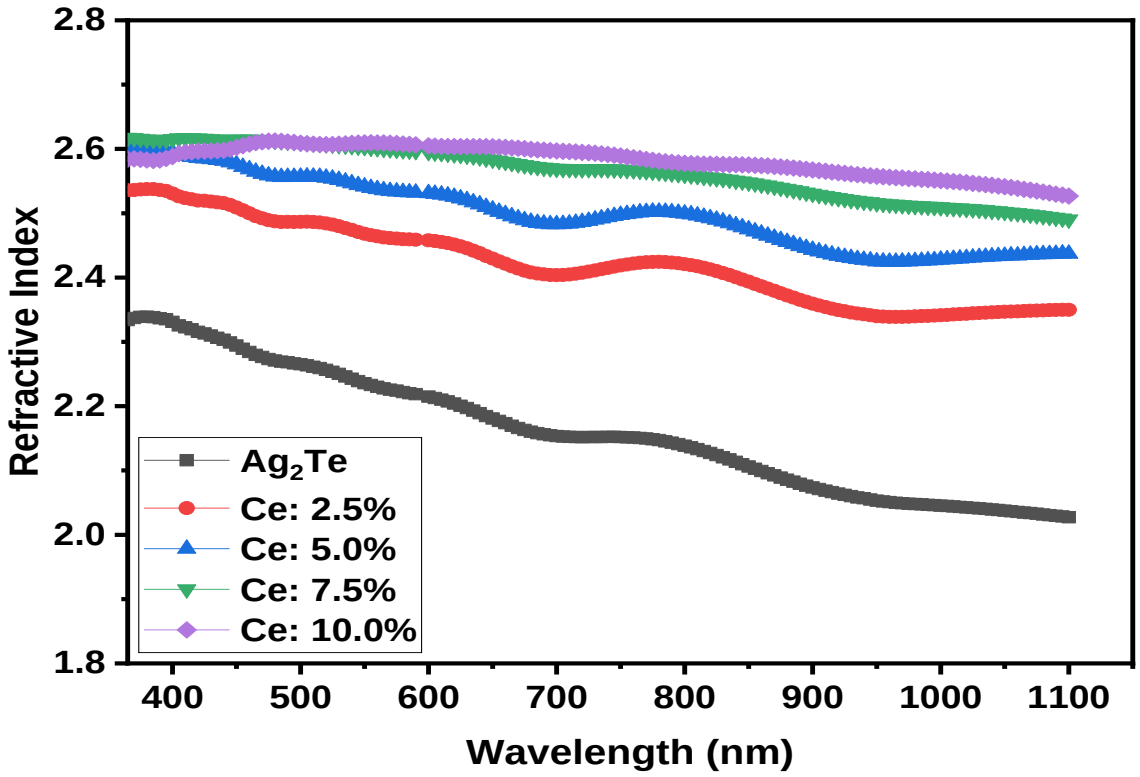

Figure 6: Plot of refractive index against wavelength for silver telluride and cerium doped silver telluride thin films deposited at different concentration of cerium ion precursor

Cerium doping significantly increases the refractive index of silver telluride thin films across all wavelengths, with higher doping concentrations resulting in progressively higher values, as shown in Figure 6. Pure Ag_2Te exhibits a decreasing refractive index from 2.33 in the UV region to 2.15 in the visible region and 2.03 in the NIR region, while doped films maintain higher values. At 2.5% cerium doping, the refractive index is 2.53 in the UV, 2.40 in the visible, and 2.35 in the NIR, while at 5.0% doping, it is 2.60 in the UV, 2.58 in the visible, and 2.43 in the NIR. For 7.5% doping, the refractive index values are 2.61, 2.57, and 2.52 in the UV, visible, and NIR regions, respectively, whereas at the highest doping level of 10.0%, the values reach 2.58, 2.60, and 2.58. The reduced wavelength dependence of the refractive index in doped films suggests improved optical uniformity and minimized free carrier absorption. Higher refractive indices enhance light confinement, making these films suitable for optical coatings and photonic applications.

ISSN 2278-2540 | DOI: 10.51583/IJLTEMAS | Volume XV, Issue VI, June 2026

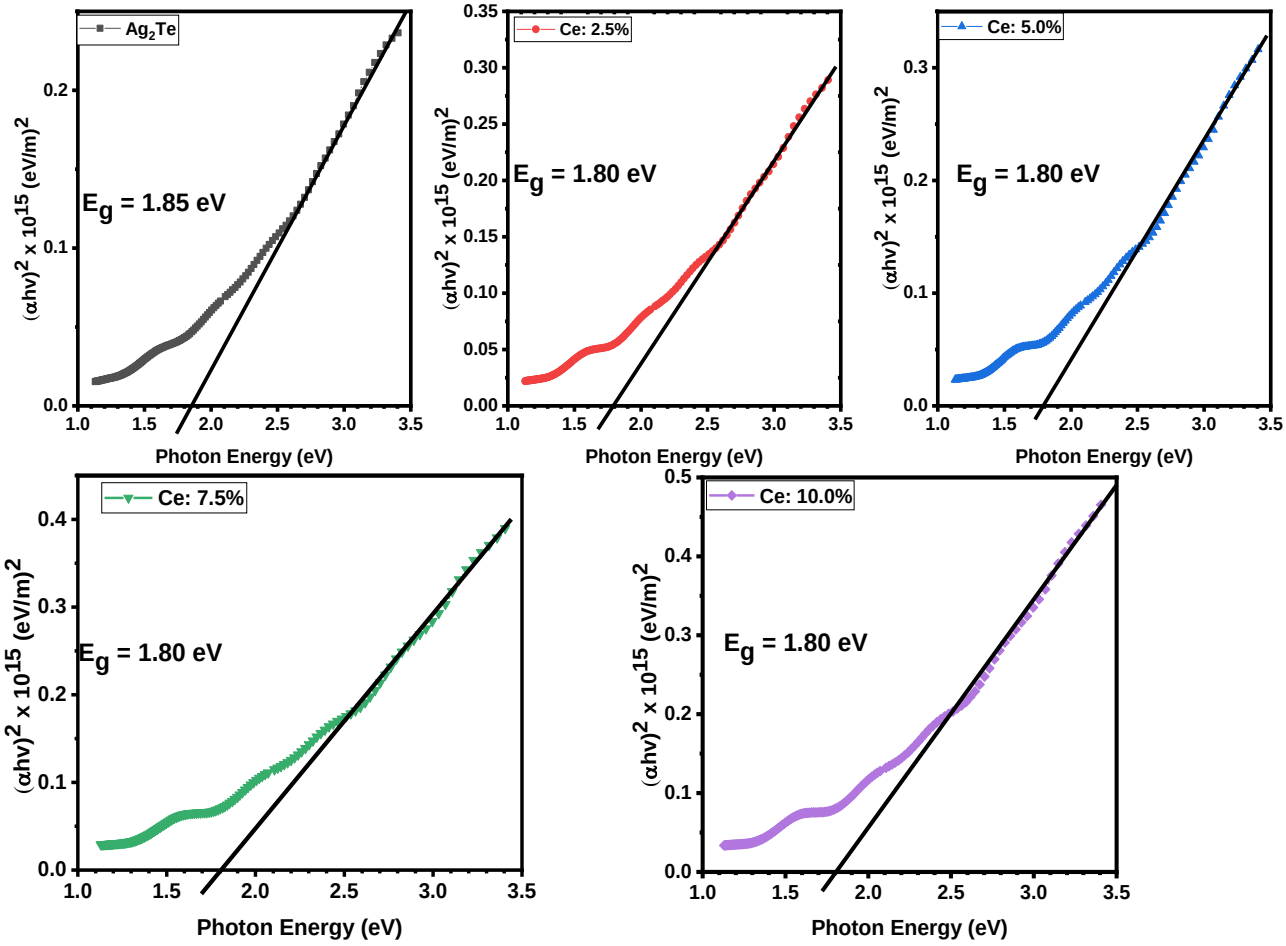

Figure 7: Plot of $(ahv)^2$against photon energy for silver telluride and cerium doped silver telluride thin films deposited at different concentration of cerium ion precursor

Figure 7 shows the plot of $(ahv)^2$against photon energy for silver telluride and cerium doped silver telluride thin films deposited at different concentration of cerium ion precursor**.** The energy band gap (E_g) of silver telluride and cerium-doped silver telluride thin films decreases slightly with cerium doping. Pure Ag_2Te has the highest band gap of 1.85 eV, indicating a wider energy range required for electron excitation. With cerium doping at 2.5%, the band gap reduces to 1.80 eV, showing a shift towards lower energy levels, which remains consistent for higher doping levels of 5.0%, 7.5%, and 10.0%, all exhibiting an E_g of 1.80 eV. This reduction suggests that cerium incorporation introduces localized states within the band structure, enhancing light absorption in lower energy regions. The narrowing of the band gap in doped films improves optical absorption in the visible and near-infrared regions, making them more efficient for optoelectronic applications. A lower band gap generally enhances the material's photoconductivity, making cerium-doped films suitable for photodetector and solar cell applications. The nearly constant E_g at higher doping levels suggests a saturation effect, where additional cerium does not significantly alter the electronic band structure. Overall, the controlled tuning of the band gap with cerium doping makes these films promising for applications requiring specific optical absorption properties.

ISSN 2278-2540 | DOI: 10.51583/IJLTEMAS | Volume XV, Issue VI, June 2026

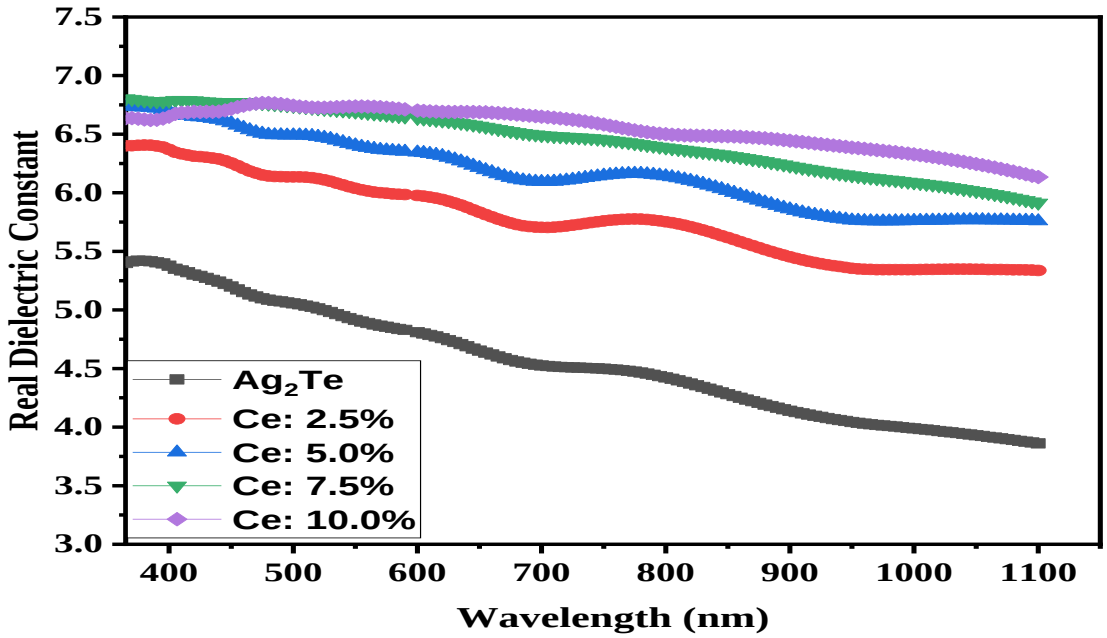

Figure 8: Plot of real dielectric constant against wavelength for silver telluride and cerium doped silver telluride thin films deposited at different concentration of cerium ion precursor

The real dielectric constant (ε_r) of silver telluride and cerium-doped silver telluride thin films, as shown in Figure 8, increases with cerium doping and decreases with increasing wavelength. Pure Ag_2Te exhibits a dielectric constant of 5.40 at 365 nm, which gradually declines to 3.86 at 1100 nm, indicating reduced polarization response at longer wavelengths. Cerium doping significantly enhances ε_r with the 2.5% doped sample showing values of 6.40 at 365 nm and 5.34 at 1100 nm. Higher doping levels of 5.0%, 7.5%, and 10.0% further increaseε_r, reaching maximum values of 6.74, 6.80, and 6.64 at 365 nm, respectively. The higher dielectric constant in doped films suggests increased charge carrier density and stronger optical interaction. The observed trend of increasing $\varepsilon_r$with decrease in wavelength aligns with the behavior of refractive index, reinforcing the correlation between optical dispersion and dielectric response. The stabilization of $\varepsilon_r$at higher doping concentrations indicates a saturation effect in polarization enhancement. A higher dielectric constant improves optical confinement, making these films suitable for applications in photonic and optoelectronic devices.

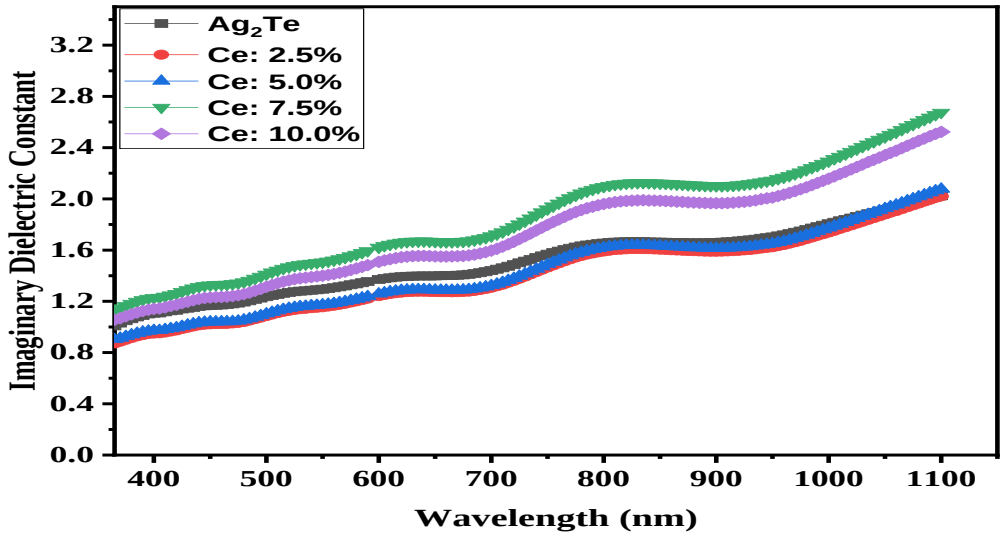

Figure 9: Plot of imaginary dielectric against wavelength for silver telluride and cerium doped silver telluride thin films deposited at different concentration of cerium ion precursor

ISSN 2278-2540 | DOI: 10.51583/IJLTEMAS | Volume XV, Issue VI, June 2026

The imaginary dielectric constant (ε_i) of silver telluride and cerium-doped silver telluride thin films, as shown in Figure 9, increases with wavelength, indicating enhanced optical losses at longer wavelengths. For pure Ag_2Te, ε_i increases from 1.01 at 365 nm to 2.02 at 1100 nm, reflecting stronger absorption in the infrared region. At 2.5% cerium doping, $\varepsilon_i$is lower at 0.87 at 365 nm but reaches 2.02 at 1100 nm, suggesting reduced absorption in the UV but similar losses in the infrared. The 5.0% doped sample follows a similar trend, with ε_i increasing from 0.90 at 365 nm to 2.08 at 1100 nm. The 7.5% doped film exhibits the highest absorption enhancement, with values of 1.13 at 365 nm and 2.67 at 1100 nm, indicating significant influence of cerium doping on absorption behavior. The 10.0% doped sample shows ε_i values of 1.06 at 365 nm and 2.52 at 1100 nm, slightly lower than the 7.5% sample but still higher than undoped Ag_2Te. The increased $\varepsilon_i$at longer wavelengths for doped films suggests enhanced free carrier absorption due to doping-induced charge carriers. The tunability of ε_i with doping concentration makes these films suitable for optoelectronic applications where controlled absorption is essential.

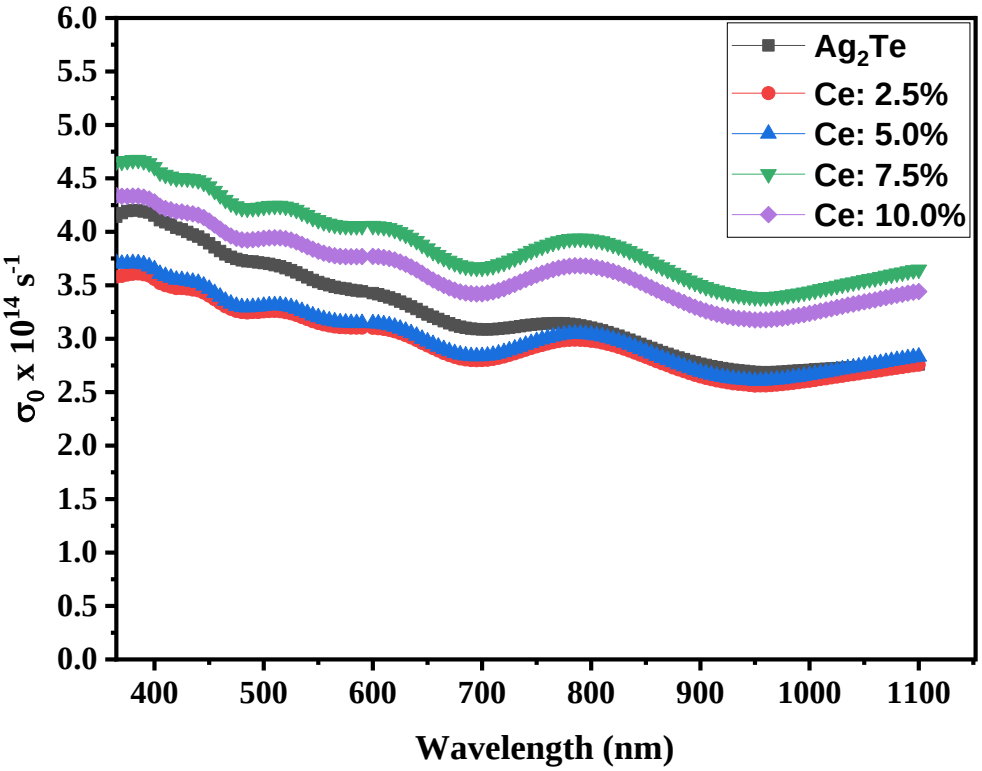

Figure 10: Plot of optical conductivity against wavelength for cerium doped silver telluride thin films deposited at different concentration of cerium ion precursor

The optical conductivity (σ_o) of silver telluride and cerium-doped silver telluride thin films, as shown in Figure 10, decreases with increasing wavelength, indicating a decline in charge carrier excitation at longer wavelengths. For pure Ag_2Te, σ_o is 4.14×10^{14} s^{-1} at 365 nm and reduces to 2.76×10^{14} s^{-1} at 1100 nm, showing significant optical response in the UV region. At 2.5% cerium doping, σ_o starts at 3.58×10^{14} s^{-1} at 365 nm and slightly decreases to $2.76 \times 10^{14} s^{-1}$ at 1100 nm, indicating reduced conductivity compared to pure Ag_2Te. The 5.0% doped sample follows a similar trend, with values of 3.71×10^{14} s^{-1} at 365 nm and 2.83×10^{14} s^{-1} at 1100 nm, suggesting a minor improvement in charge transport. The 7.5% doped film exhibits the highest conductivity enhancement, with σ_o increasing to 4.66×10^{14} s^{-1} at 365 nm and maintaining a higher value of 4.65×10^{14} s^{-1} at 1100 nm, demonstrating significant doping influence. The 10.0% doped sample shows σ_o values of 4.34×10^{14} s^{-1} at 365 nm and 4.21×10^{14} s^{-1} at 1100 nm, slightly lower than the 7.5% sample but still higher than undoped Ag_2Te. The higher optical conductivity in doped films, particularly at 7.5%, suggests enhanced free carrier generation due to cerium incorporation. The declining trend with wavelength indicates that the films are more optically active in the UV-visible region. The improved conductivity at higher doping levels enhances the potential of these materials for optoelectronic applications, such as photodetectors and transparent conductive coatings

ISSN 2278-2540 | DOI: 10.51583/IJLTEMAS | Volume XV, Issue VI, June 2026

CONCLUSION

Thin films of silver telluride (Ag_2Te), and cerium-doped silver telluride (Ce: Ag_2Te) were successfully deposited on fluorine-doped tin oxide (FTO) glass substrates using the electrodeposition technique. The precursors used for the deposition included aqueous solutions of silver trioxonitrate (V), cerium tetraoxosulphate (VI) tetrahydrate, and tellurium (IV) oxide, which served as sources of Ag, Ce, and Te, respectively. Ethylene diamine tetra acetic acid (EDTA) was employed as a complexing agent, while tetraoxosulphate (VI) acid was used to adjust the pH of the electrolyte bath. Cerium ions were incorporated as dopants into Ag_2Te matrices. Deposition parameter such as dopant concentration (0–10%),was systematically optimized to study their effects on the film optical properties.

Optical characterization using UV-Vis-NIR spectroscopy showed that absorbance improved significantly with cerium doping. For example, absorbance at 365 nm increased from 33.46% to 39.35% in Ag_2Te. Corresponding transmittance values decreased, indicating enhanced optical density. Reflectance increased slightly, reaching a maximum of approximately 20.3%. Extinction coefficients ranged between 1.26×10^{-1} and 1.83×10^{-1}, while refractive indices varied from 2.42 to 2.63. Dielectric constants (real and imaginary), optical conductivity, and other derived optical functions also showed enhancements with doping. The optical band gaps narrowed with increasing cerium content from 1.61 to 1.34 eV in Ag_2Te, indicating improved light absorption in the visible to near-infrared region.

REFERENCES

1. Nande, A., Kalyani, N. T., Tiwari, A., & Dhoble, S. J. (2023). Exploring the world of functional materials. In Functional Materials from Carbon, Inorganic, and Organic Sources. Woodhead Publishing Series in Electronic and Optical Materials. Woodhead Publishing, pp. 1–19.
2. Sousan Gholamrezael, Masoud Salavati Niasari, Davood Ghanbari, & Samira Bagheri. (2016). Hydrothermal preparation of silver telluride nanostructures and photo-catalytic investigation in degradation of toxic dyes. Scientific Reports, 6, Article 20060.
3. Akhil Sreevalsan, Gunhee Kim, Yifan Yu, & Sujoy Bandyopadhyay. (2025). Ag_2Te quantum dots: Emerging heavy metal-free chalcogenides for near and shortwave infrared photodetectors. ACS Applied Electronic Materials, 7(21), 9623–9642.
4. Ha Heun Lee, Subin Lee, Geunwoo Hwang, Seungyeon Lee, & Suyeon Cho. (2024). Vapor-liquid-solid synthesis of Ag_2Te using chemical vapor deposition method. APL Materials, 12, 011123.
5. Nonso Livinus Okoli, Laz Nnadozie Ezenwaka, Ngozi Agatha Okereke, Ifeyinwa Amaka Ezenwa, & Nwode Augustine Nwori. (2022). Investigation of optical, structural, morphological and electrical properties of electrodeposited cobalt doped copper selenide ($Cu_{1-x}Co_xSe$) thin films. Trends in Sciences, 19(16), 5686.
6. Laia Ferrer-Argemi, Ziqi Yu, Jiwon Kim, Nosang V. Myung, & Jae-Hong Lim. (2019). Silver content dependent thermal conductivity and thermoelectric properties of electrodeposited antimony telluride thin films. Scientific Reports, 9, Article 9242.
7. Alaa M. Abd-Elnaiem, A. M. Abdelraheem, M. A. Abdel-Rahim, & Samar Moustafa. (2022). Substituting silver for tellurium in selenium–tellurium thin films for improving the optical characteristics. Journal of Inorganic and Organometallic Polymers and Materials, 32, 2009–2021.
8. Gupta, S. (2025). High Performance Silver Telluride Thin Films: An Experimental Study. First Edition. Scholarly Publication.
9. Penglu Yu, Mingxuan Li, Wenqian Lv, Zhilei Liu, & Shangheng Yu. (2025). Iodide ion-assisted silver-telluride-based nanowires: Morphology optimization and efficient doping for improved thermoelectric application. Nano-Micro Small, 21(15).
10. Gode, F., Kariper, I. A., Guneri, E., & Unlu, S. (2017). Effect of complexing agents on the structural, optical and electrical properties of polycrystalline indium sulphide thin films deposited by chemical bath method. Acta Physica Polonica A, 132(3), 527–530.
11. Gode, F., & Unlu, S. (2018). Nickel doping effect on the structural and optical properties of indium sulfide thin films by SILAR. Open Chemistry, 16, 757–762.

ISSN 2278-2540 | DOI: 10.51583/IJLTEMAS | Volume XV, Issue VI, June 2026

12. Chaudhary, P., & Kumar, V. (2019). Preparation of ZnO thin film using sol-gel dip-coating technique and their characterization for optoelectronic applications. World Scientific News, 121, 64–71.
13. Lokhande, C. D., Sankapal, B. R., Mane, R. S., Pathan, H. M., Muller, M., Giersig, M., & Ganesan, V. (2002). XRD, SEM, AFM, HRTEM, EDAX and RBS studies of chemically deposited Sb_2S_3 and Sb_2Se_3 thin films. Applied Surface Science, 193(1), 1–10.
14. Ismail, B., Mushtaq, S., & Khan, A. (2014). Enhanced grain growth in the Sn doped Sb_2S_3 thin film absorber materials for solar cell applications. Chalcogenide Letters, 11(1), 37–45.
15. Augustine, Nnabuchi, Chikwenze, M. N., Anyaegbunam, R. A., F. N. C., Kalu, P. N., Robert, B. J., Nwosu, C. N., Dike, C. O., & Taddy, E. N. (2019). Comparative investigation of some selected properties of Mn_3O_4/PbS and CuO/PbS composites thin films. Materials Research Express, 6(066416), 1–10.
16. Guneri, E. (2019). The role of Au doping on the structural and optical properties of Cu_2O films. Journal of Nano Research, 58, 49–67.
17. Suresh Sagadevan, & Isha Das. (2017). Chemical bath deposition (CBD) of zinc selenide (ZnSe) thin films and characterization. Australian Journal of Mechanical Engineering, 15(3), 222–227.
18. Bekkari, R., Jaber, B., Labrim, H., Quafi, M., Zayyoun, N., & Laahab, L. (2019). Effect of solvents and stabilizer molar ratio on the growth orientation of sol-gel derived ZnO thin films. International Journal of Photoenergy, 2019(3164043), 1–7.
19. Abouda, A. A., Mukherjeeb, A., Revaprasaduc, N., & Mohamed, A. N. (2019). The effect of Cu-doping on CdS thin films deposited by the spray pyrolysis technique. Journal of Materials Research and Technology, 8(2), 2021–2030.
20. Tezel, F. M., Ozdemir, O., & Kariper, I. A. (2017). The effects of pH on structural and optical characterization of iron oxide thin films. Surface Review and Letters, 24(4), 1750051, 1–10.
21. Ongwen, N. O., Oduor, A. O., & Ayieta, E. O. (2019). Effect of concentration of reactants on the optical properties of iron-doped cadmium stannate thin films deposited by spray pyrolysis. American Journal of Materials Science, 9(1), 1–7.
22. Sreedev, P., Rakhesh, V., & Roshina, N. S. (2018). Optical characterization of ZnO thin films prepared by chemical bath deposition method. IOP Conference Series: Materials Science and Engineering, 377, 012086, 1–7.
23. Guneri, E., & Kariper, A. (2018). Characterization of high quality chalcogenide thin films fabricated by chemical bath deposition. Electronic Materials Letters, 9(1), 13–17.
24. Augustine, Nnabuchi, Chikwenze, M. N., Anyaegbunam, R. A., F. N. C., Kalu, P. N., Robert, B. J., Nwosu, C. N., Dike, C. O., & Taddy, E. N. (2019). Comparative investigation of some selected properties of Mn_3O_4/PbS and CuO/PbS composites thin films. Materials Research Express, 6(066416), 1–10.
25. Kariper, I. A. (2018). A new route to synthesis MnSe thin films by chemical bath method. Materials Research, 21(2), 1–6.
26. Mushtaq, S., Tahir, S. A., Ashfaq, A., Ahmad, W., & Baig, A. (2022). Effect of ammonia on the structural, morphological and optical properties of nanocrystalline ZnS thin film. Optik, 261, 169088.